JOURNAL OF Applied Polymer SCIENCE

Effect of Nano-silica on the Mechanical, Thermal, and Crystalline Properties of Poly(vinyl alcohol)/Nano-silica Films

Chao Wang,[1] Jingwei Wei,[2] Bingxiang Xia,[2] Xian Chen,[1] Bobing He[1]

[1]Polymer Physics and Chemistry, College of Chemistry, Sichuan University, Chengdu 610064, China

[2]Department of Materials Processing Engineering, College of Polymer Science and Engineering, Sichuan University, Chengdu 610065, China

Correspondence to: B. He (E-mail: hbbeyou@163.com) or X. Chen (E-mail: xian.chen@126.com)

ABSTRACT: Poly(vinyl alcohol)/nano-silica (PVA/nano-SiO_2) films were prepared through extrusion blowing with the addition of water and glycerin as plasticizer. The characteristic properties of PVA/nano-SiO_2 films were investigated by differential scanning calorimetry, dynamic mechanical analysis, Haake torque rheometry, and atomic force microscopy (AFM). The results showed that the mechanical properties of PVA/nano-SiO_2 were improved dramatically. The tensile strength of the nanofilms increased from 62 MPa to 104 MPa with loading 0.3 wt % nano-SiO_2 and the tear strength was improved from 222 KN/m to 580 KN/m. The crystallinity of the films loaded with 0.4 wt. % nano-SiO_2 decreased from 32.2% to 21.0% and the AFM images indicated that the amorphous region of nanofilms increased with increasing nano-SiO_2 content. The storage modulus and loss modulus increased to two and nearly three times with 0.3 wt % nano-SiO_2 loading. © 2012 Wiley Periodicals, Inc. J. Appl. Polym. Sci. 000: 000–000, 2012

KEYWORDS: films; nanoparticles; nanowires and nanocrystals; thermal properties; crystallization; crosslinking

Received 23 March 2012; accepted 30 June 2012; published online

DOI: 10.1002/app.38277

INTRODUCTION

In recent years, poly(vinyl alcohol) (PVA) incorporated with nanoparticles have drawn much attention because of the excellent properties of nanofillers. The properties of the PVA nanocomposites, such as mechanical and thermal properties, have been improved dramatically due to the nano-size structure, surface characteristics of nanofillers, and the interactions between PVA matrix and nanofillers. Many kinds of nanoparticles have been added into PVA matrix, such as metal,[1] metal oxide,[2–4] metal sulfide,[5–7] silica,[8] montmorillonite,[9,10] carbon-based nanoparticles,[11–13] and organic nanoparticles,[14,15] to improve the properties of PVA.

Among the nanoparticles mentioned above, oxide nanoparticles have good applications on modifying PVA. Sirirat Wacharawichanant et al.[2] prepared PVA/vanadium pentoxide (V_2O_5) nanocomposites by solution mixing. The results showed the improvement of the tensile strength, Young's modulus and stress at break by adding V_2O_5. And the degradation temperature of the PVA/V_2O_5 nanocomposites increased with increasing V_2O_5 content. Lou et al.[16] prepared PVA/titanium dioxide (TiO_2) nanocomposites with surface-carboxylated nano-TiO_2 by a solution-blend film-casting method. They found a great improvement of tensile strength on the nanocomposites. With increasing carboxylated nano-TiO_2 content, the storage modulus increased and loss tangent decreased. Guo et al.[17] studied PVA-silica nanocomposite membranes prepared under catalyzed sol-gel reaction of γ-mercaptopropyltrimethoxysilane within PVA matrix. The results indicated that nanoscale silica homogeneously distributed in PVA matrix and the thermal stability was significantly enhanced. D.M. Fernandesa et al.[18] investigated the characterization of PVA/zinc oxide(ZnO) nanocomposite films. It was found that interactions between PVA and ZnO existed in some compositions. The crystallinity of PVA increased with UV irradiation and the presence of ZnO. The roughness of PVA/ZnO films increased after 96 h UV irradiation. Gandhi et al.[19] researched the effect of nickel oxide (NiO) on PVA/NiO nanocoposite. The resulting PVA/NiO nanocomposite became amorphous because of the reactions between NiO and PVA. The thermal stability of PVA/NiO nanocomposite was improved with the increasing NiO content.

PVA material has excellent gas barrier properties, flexibility, transparency, and toughness. Therefore, PVA has been developed as a barrier film for food packaging application.[20–23] Moreover, PVA can be produced through a nonpetroleum route, which makes PVA very important under the situation of petroleum scarcity.[24] In this study, nano-SiO_2 was selected to

enhance the properties of PVA due to the unique properties of nano-SiO_2, such as large specific surface area, light weight, high dispersion into matrix. Furthermore, nano-SiO_2 has great improvement on mechanical properties, storage modulus, and loss modulus of matrix with lower addition compared with other nanofillers.

The previous researches mentioned above almost prepared the PVA nanocomposites by an aqueous solution method. In this study, PVA/nano-SiO_2 films were prepared through extrusion blowing. And glycerin and water were added into PVA as plasticizer to broaden the temperature window between the melting point and its decomposition temperature.[25–27] Compared with traditional aqueous solution method, extrusion blowing method can save much energy and time.[28] This article focused on the thermal behavior, the dynamic mechanical, rheological, and mechanical properties, and, in particular, crystalline behavior of PVA films loaded with different content of nano-SiO_2.

EXPERIMENTAL

Materials

A commercial grade of PVA was provided by Kuraray (Japan) in granule form: PVA 117, degree of polymerization = 1700, hydrolysis = 99.0–99.8 mol %, density = 1.19 g/cm^3. The nano-SiO_2 was obtained by Guangdong Jibisheng (China) in powder form: density = 0.04–0.06 g/cm^3, hydrophobic nano-SiO_2 (HB 215, specific surface area = 115 ± 15 m^2/g), hydrophilic nano-SiO_2 (HL150, specific surface area = 150 ± 15 m^2/g). The industrial glycerin, density = 1.26 g/cm^3, which was supplied by Kao Corporation (Japan), was used as a plasticizer. Deionized water, which was also a plasticizer, was commercial grade.

Sample Preparation

The PVA raw material was washed with deionized water to neutral and dried in oven at 70°C for 12 h. Then 15 wt % glycerin and 15 wt % deionized water were added into the dried PVA. The blends were mixed in a high speed mixer (GH-10DQ, Beijing Plastic Machinery Factory, Beijing, China) for about 10 min under 70°C. Pellets were prepared by granulating the extrudates produced by a Haake twin-screw extruder (Haake-Rheocord 9000, Germany) with a 20 mm diameter and L/D ratio of 25. The screw speed and barrel temperatures of the extruder were 50 rpm and 200–225°C. PVA films were then prepared by a Haake extrusion blowing machine (extrusion die diameter: 30 mm; die gap: 1 mm; inflation rate: 1.5) to produce the films with the same thickness, each with different content of nano-SiO_2.

Haake Torque Measurement

The prepared blends (70 g) were mixed in Haake rheometer for 8 min at 50 rpm/min at 200°C. The torque curve changing with time was recorded.

Mechanical Properties Measurements

The tensile properties and tear strength of the films were measured by a universal testing machine (Instron 4302). The tensile properties were measured at a crosshead speed of 20 mm/min according to ASTM D638, while the tear strength was measured at a crosshead speed of 200 mm/min according to ASTM D1004-09. The hardness test was carried out with a Shore Durometer according to ASTM D2240. For all of the above tests, a minimum of five samples were used for each blend series and the average values calculated.

Differential Scanning Calorimetry

Thermal properties were investigated by the Netzsch-DSC-204 differential scanning calorimeter (Germany). The samples weighing 8 mg were placed in aluminum crucibles and were first kept in the molten state at 250°C for 3 min to erase the thermal history and then cooled down to room temperature at 20°C/min. The whole process was under nitrogen atmosphere. The sample crystallinity was calculated as $X(\%)=\Delta H_f/\Delta H_f^0\times 100\%$, where ΔH_f is the melting enthalpy of PVA. ΔH_f^0 is the melting enthalpy of PVA at 100% crystallization, 168 J/g.[29]

Dynamic Mechanical Analysis

The sample specimens (30 × 10 × 0.04 mm^3) were analyzed by DMA-2980 dynamic mechanical analyser (TA Instruments). The scanning temperature range was selected from −20°C to 90°C at a rate of 3°C/min and the stretching mode was chosen with 1 Hz frequency.

Atomic Force Microscopy

Blowing films with smooth surface and consistent thickness were selected to observe the crystalline morphology of the PVA. The atomic force microscopy (AFM) measurements were performed with a NanoScope Multimode SPM (Vecco Instruments). All phase imaging was performed in the tapping mode to avoid surface damage, and the AFM images (1μm scans) were acquired by scanning the sample in air under ambient laboratory conditions (25°C).

RESULTS AND DISCUSSION

Processing Properties

The effects of different content of hydrophobic and hydrophilic nano-SiO_2 on the processing properties of PVA were shown in Figures 1 and 2. The results plotted in Figure 1 indicate that the processing viscosity of the PVA was hardly influenced by the addition of the hydrophobic nano-SiO_2. However, as shown in Figure 2, the processing properties of PVA changed greatly with the increase of hydrophilic nano-SiO_2. The balance torque of the system increased from 24 N·M to 30 N·M by adding 0.05 wt % nano-SiO_2. When the content of the hydrophilic nano-SiO_2 was increased to 0.3 wt %, the balance torque increased to 52 N·M. The significant increase of balance torque may be attributed to the entanglement network, which resulted from the hydroxyl interactions between hydrophilic nano-SiO_2 and PVA molecules. As the content of the hydrophilic nano-SiO_2 increased, the number of junction-point of the entanglement network increased. Therefore, the viscosity of the system increased rapidly. In terms of the above observation, the hydrophilic nano-SiO_2 was selected in the following discussions.

Mechanical Properties

Figure 3 shows the effect of nano-SiO_2 content on the mechanical properties of PVA/nano-SiO_2 films. There was a general increase in the tensile strength and tear strength of the PVA films when the nano-SiO_2 content increased. The tensile strength of the nanofilms increased from 62 MPa to 104 MPa with the increase of nano-SiO_2, indicating that the PVA was strengthened by the improvement of interfacial adhesion, as

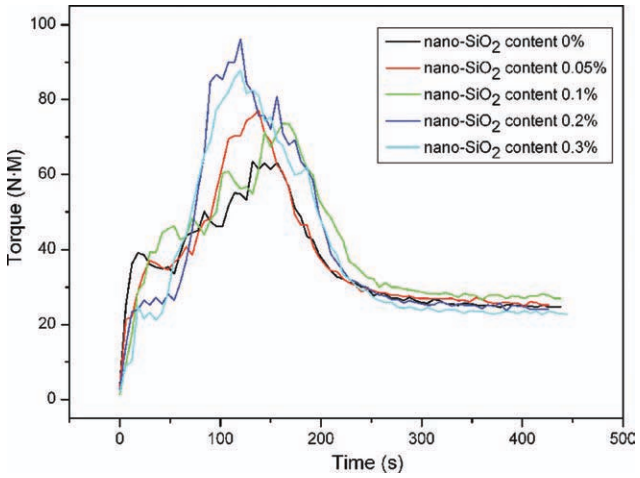

Figure 1. Curves of torque versus time in the Haake torque rheometer of neat PVA and PVA/hydrophobic nano-SiO_2. [Color figure can be viewed in the online issue, which is available at wileyonlinelibrary.com.]

reported by Xiangmin Xu.[30] Due to the interactions between nano-SiO_2 and PVA, the nano-SiO_2 particles are easily adhered to PVA molecular chains. As a result, the tensile strength was enhanced. But the increasing trend slowed down when the content of nano-SiO_2 increased beyond 0.2 wt %. Because the interactions between nano-SiO_2 and PVA gradually tended to saturation. The tear strength, which was improved from 222 KN/m to 580 KN/m, increased nearly two times. The hardness increased from 72 to 82 by adding 0.3 wt % nano-SiO_2. It has been reported that an improvement of both the strength and stiffness result from the existence of an interface structure between filler and matrix based on both hydrogen bonding and covalent bonding for silica/nylon 66 composites.[30] To the contrary, the elongation at break decreased from 230%to 100% with the nano-SiO_2 content increasing to 0.3 wt %. It is resulted from the rigidity of the inorganic nanoparticles and the formation of entanglement network. The significant change in

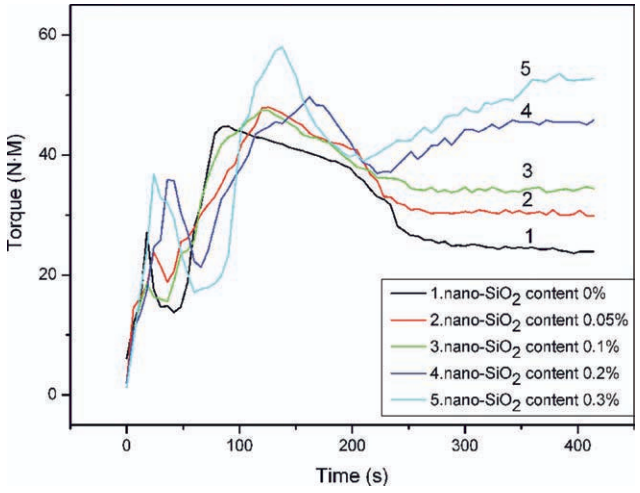

Figure 2. Curves of torque versus time in the Haake torque rheometer of neat PVA and PVA/hydrophilic nano-SiO_2. [Color figure can be viewed in the online issue, which is available at wileyonlinelibrary.com.]

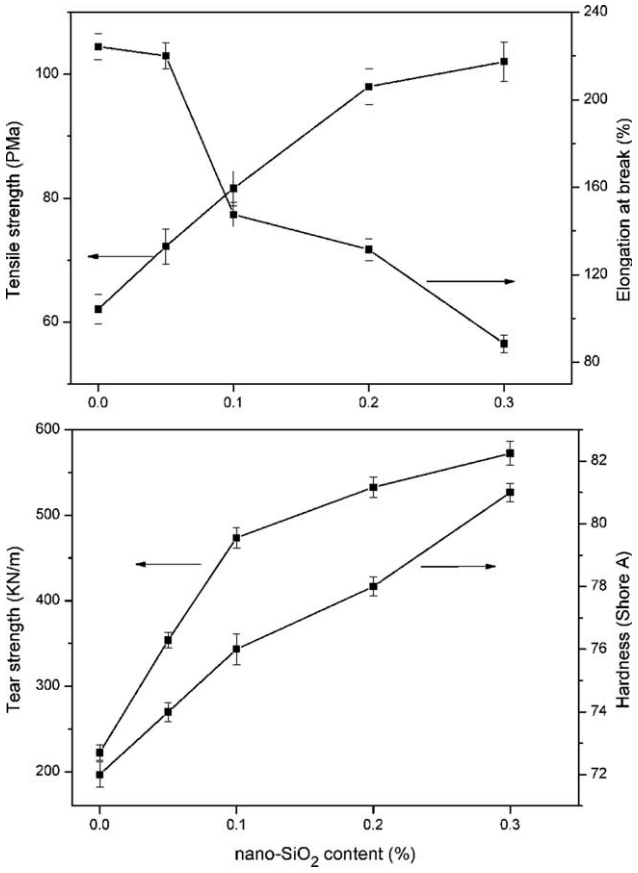

Figure 3. Tensile strength (MPa), elongation at break (%), tear strength (KN/m), and hardness (Shore A) of PVA and PVA/nano-SiO_2 nanofilms.

mechanical properties of PVA illustrates that nano-SiO_2 plays an important role in modifying PVA matrix. With increasing content of nano-SiO_2, the hydroxyl interactions and the physical adsorption between PVA and nano-SiO_2 improved simultaneously. In other words, the molecular interaction within PVA and nano-SiO_2 was reinforced. This is in agreement with the observation of the balance torque.

Thermal Properties

To analyze the effect of nano-SiO_2 content on the crystalline behaviors of PVA nanofilms, the melting temperature and the degree of crystallinitiy of the different samples are presented in Table I. Compared with the neat PVA, no significant changes in melting temperatures were observed after adding different amount of nano-SiO_2. The enthalpy of the films decreased from

Table I. Melting Parameters of PVA Systems with Different Nano-SiO_2 Content.

Nano-SiO_2 content (%)	Enthalpy (J g^{-1})	Melting point (°C)	Crystallinity (%)
0.0	54.2	212.5	32.2
0.1	47.8	211.6	28.5
0.2	38.4	212.9	22.8
0.4	33.3	211.3	21.0

54.2 J/g to 33.3 J/g with loading 0.4 wt % nano-SiO_2. The crystallinity also decreased with increasing nano-SiO_2 content. For neat PVA, the crystallinity was 32.2%. As the content of nano-SiO_2 increased from 0.1 wt % to 0.4 wt %, the crystallinity decreased gradually from 28.5% to 21.0%. The results obtained in this study are comparable with those obtained in previous reports for other matrices.[31,32] It has been found that the crystallization process will be obstructed in the presence of nano-SiO_2. The bulk PVA possesses excellent crystallization ability due to the strongly hydroxyl interactions within the molecular chains.[33] When nano-SiO_2 was added into PVA matrix, the hydroxyl interactions occurred between PVA and nano-SiO_2 and interfered the intermolecular hydroxyl interactions of PVA to some extent. This would make the regular arrangement of folded chains to be difficult. As a result, the crystallinity of PVA decreased.

From the above results, further explanation can be given for the changes of the mechanical properties of PVA/nano-SiO_2 films. Due to the presence of the entanglement network, two phenomena occurred in the nano-systems. On one hand, the interaction between the molecules of PVA/nano-SiO_2 was reinforced. As a result, the tensile strength and the tear strength were improved. On the other hand, the decreased crystallinity would lead to slightly lower strength. However, the former aspect was presumably greater. Therefore, the mechanical proprieties of the PVA/nano-SiO_2 changed greatly.

Dynamic Mechanical Properties

The dynamic storage modulus, loss modulus and the tan δ for neat PVA and the nanofilms were measured as a function of temperature, as shown in Figure 4. According to Figure 4(a), the storage modulus of the PVA films were increased by the addition of nano-SiO_2, as expected. When increasing nano-SiO_2 content to 0.3 wt %, the storage modulus of PVA increased rapidly from 2480 MPa to 5108 MPa. The value of loss modulus peak enhanced by nearly two times, compared to neat PVA film [Figure 4(b)]. The great improvement of storage modulus and loss modulus owed to a network structure generated in the matrix by adding nanoparticles, this is consistent with related literature.[34–36] Such a crosslink for nano-SiO_2 limits the movement of the molecular chains and raises the storage modulus of the matrix. This is also the reason why the mechanical properties changed significantly as the above results showed. Of course, the crystalline behavior of PVA was influenced greatly by the entanglement network.

As illustrated in Figure 4(c), the addition of nano-SiO_2 made the glass transition temperature (T_g) of PVA films decrease from 41°C to 37°C, then to 30°C in the first instance, and increased to 36°C at last. The T_g of PVA nanofilms decreasing with increasing nano-SiO_2 content was studied in previous researches.[34,37] Sarkar et al.[34] thought that the decrease of T_g of PVA contributed to the decrease of the intermolecular hydrogen bonds between PVA and nano-SiO_2 particles. With increasing nano-SiO_2 content, more and more hydrogen bonds generated between PVA molecular chain and nano-SiO_2. The amount of intermolecular hydrogen bond of PVA reduced relatively, which resulted in the decrease of crystallinity of PVA. The decrease in crystallinity of PVA upon the addition of silica may lead to relatively easier movement of the PVA molecular chain, thus resulting in the depression of T_g of PVA. When the content of nano-SiO_2 was increased to 0.3 wt %, the T_g of PVA film increased back to 36°C. This may be associated with the strong hydroxyl interactions between PVA molecules and nano-SiO_2, which

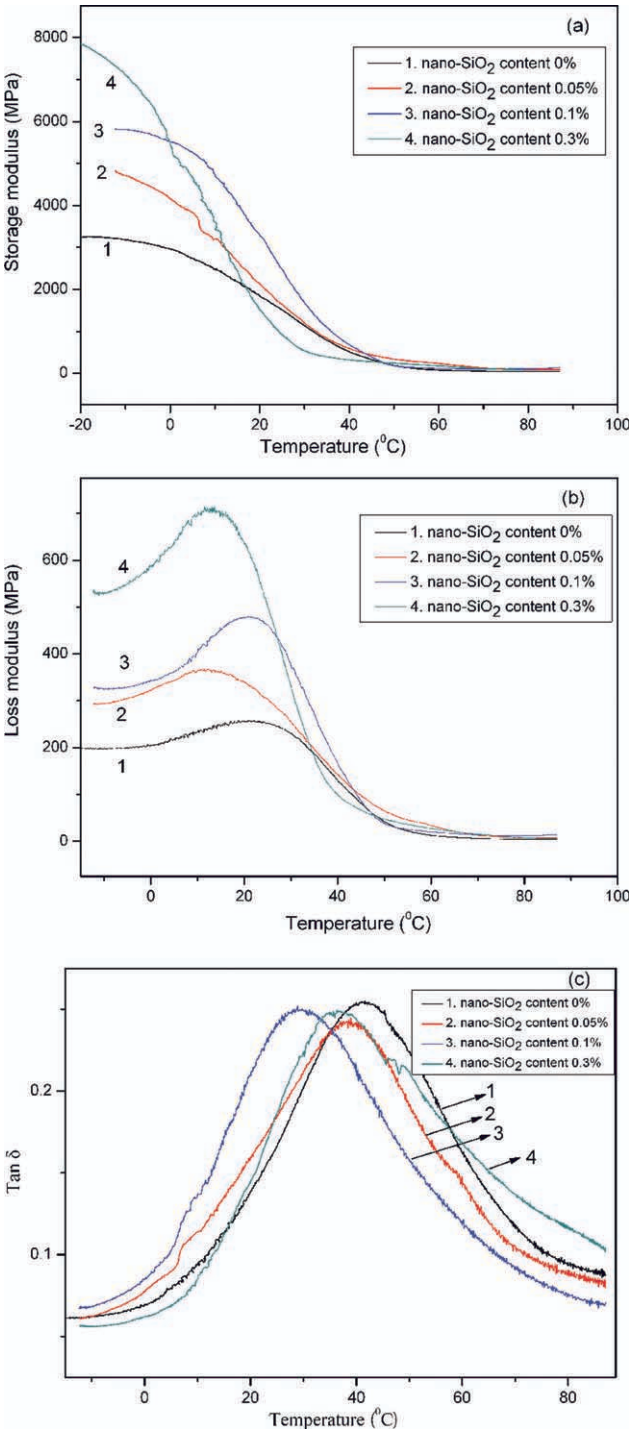

Figure 4. Dynamic mechanical analysis curves of PVA and PVA/nano-SiO_2 films. [Color figure can be viewed in the online issue, which is available at wileyonlinelibrary.com.]

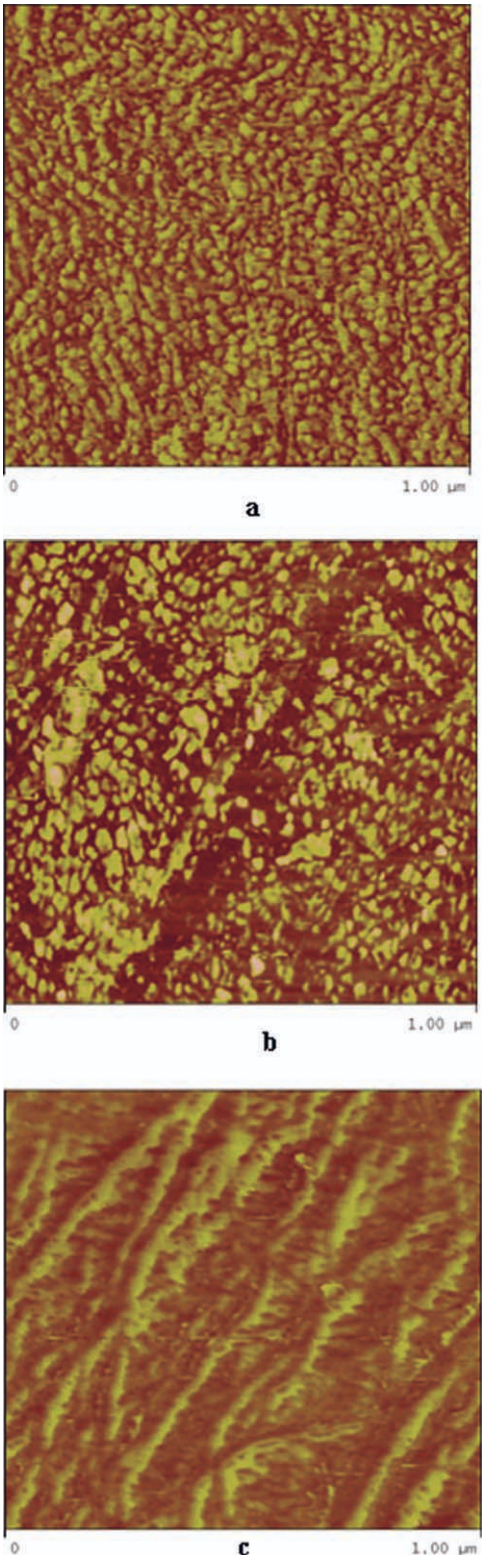

Figure 5. The surface phase imaging of PVA films with different content of nano-SiO_2. (a) PVA without nano-SiO_2; (b) PVA with 0.1 wt % nano-SiO_2; (c) PVA with 0.3 wt % nano-SiO_2. [Color figure can be viewed in the online issue, which is available at wileyonlinelibrary.com.]

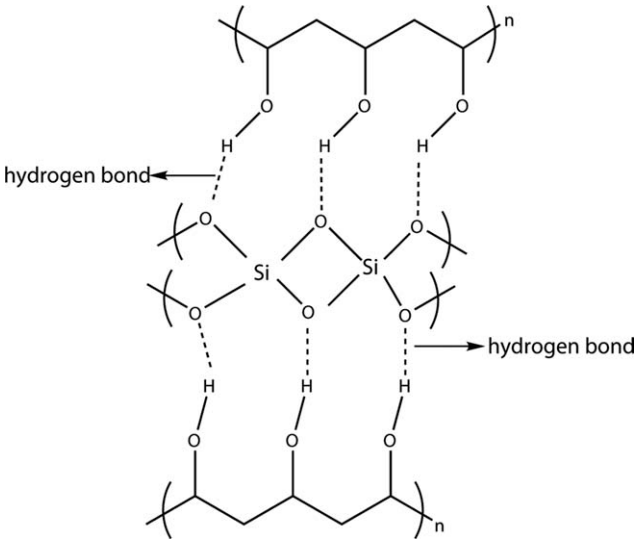

Figure 6. Structural representation of the hydrogen bond effect of nano-SiO_2.

formed the entanglement structure and restricted the movement of the PVA chains. Consequently, the T_g of PVA increased. The similar result was also reported by Wu et al.[38]

Atomic Force Microscopy Analysis

In the AFM photographs, it was not easy to determine whether the bright spot were crystals of the polymer or aggregates of the nano-SiO_2. As a result, we discuss primarily the aggregated structures corresponding to the varied amorphous phases of the AFM images. As shown in Figure 5, an obvious variation of the amorphous phase was found. Compared with Figure 5(a), the amorphous structure present in Figure 5(b) appeared to increase much. As indicated above, this was induced by the hydroxyl interactions between the molecular chains of PVA and the nano-SiO_2. The molecules of the formed network can not arrange into a crystal lattice, causing the increase of the amorphous region. Particularly for the composite with 0.3 wt % nano-SiO_2, the intermolecular reactions seemed more intensely as a result of much more amorphous area shown in Figure 5(c).

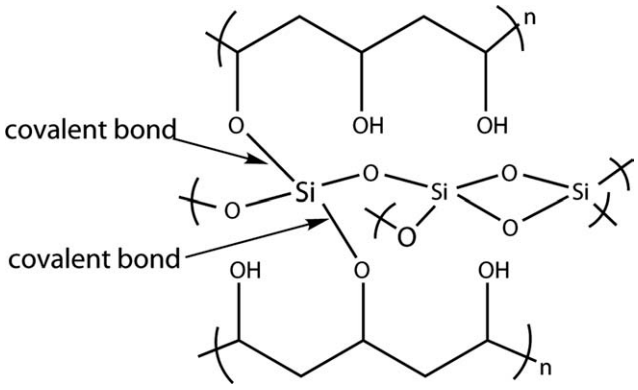

Figure 7. Structural representation of the chemical crosslink effect of nano-SiO_2.

All of the observations in the AFM were consistent with the above discussions.

According to the above discussions, the significant changes in PVA by incorporation of nano-SiO_2 are most probably attributed to the formed entanglement network. To explain this mechanism better, two schemes are proposed to show the structures.

The first one hydrogen bond presented in Figure 6. The 99% hydrolyzed PVA used in this study is a highly polar matrix containing large numbers of hydroxyl group. The hydrogen bond was likely to generate between hydroxyl and hydrophilic nano-SiO_2. The existence of hydrogen bond between PVA and hydrophilic nano-SiO_2 played an important role in improving the mechanical properties, such as tensile strength.[39] Nath et al.[40] explained the formation of hydrogen bond between PVA and silica in their study on PVA/fly ash composite films. They found that physically or chemically interactions were more likely to form between fly ash and highly polar PVA rather than nonpolar polypropene.

Figure 7 presents the other probable structure of the matrix. Because of the weak acidity of hydrophilic nano-SiO_2, a dehydration reaction may take place between nano-SiO_2 and PVA chains when the system was at high temperature. In consequence, a chemical crosslink network may be formed between PVA and nano-SiO_2. As a result, the processing viscosity and mechanical properties, as well as the other properties of PVA would be changed. This structure has been mentioned in the literature by Tang et al.[41,42] They indicated that a strong chemical bond (C—O—Si) was formed between nano-SiO_2 and PVA matrix, which were prepared through a casting method. In this article, it is considered that both of the crosslinks occur in the PVA/nano-SiO_2 films and chemical crosslink is the major one because of the great changes of the properties of PVA nanofilms.

CONCLUSION

The PVA/nano-SiO_2 films prepared through extrusion blowing were studied in this article. The results showed that the viscosity of PVA increased obviously with the increasing content of hydrophilic nano-SiO_2. With loading 0.3 wt % nano-SiO_2, the tensile strength of the nanofilms increased from 62 MPa to 104 MPa and the tear strength was improved from 222 KN/m to 580 KN/m. For the thermal properties, the crystallinity of the film loaded with 0.4 wt % nano-SiO_2 decreased from 32.2% to 21.0%. According to the AFM figures, the crystallization area of modified PVA reduced, and the regularity of the crystal decreased. In addition, the storage modulus and loss modulus increased to two and nearly three times with 0.3 wt % nano-SiO_2 loading. In a word, the properties of PVA film prepared through extrusion blowing were greatly improved by adding nano-SiO_2 and it will be a good idea to enhance the properties of PVA.

REFERENCES

1. Ananth, A. N.; Umapathy, S.; Sophia, J.; Mathavan, T.; Mangalaraj, D. *Appl. Nanosci.* **2011,** *1*, 87.
2. Wacharawichanant, S.; Wutanasiri, N.; Srifong, P.; Meesangpan, U.; Thongyai, S. *J. Appl. Polym. Sci.* **2011,** *121*, 2876.
3. Mallakpoura, S.; Baratia, A. *Prog. Org. Coat.* **2011,** *71*, 391.
4. Maurya, A.; Chauhan, P. *Polym. Bull.* **2012,** *68*, 961.
5. Saikiaa, D.; Saikiab, P. K.; Gogoic, P. K.; Dasd, M. R.; Senguptad, P.; Shelkee, M. V. *Mater. Chem. Phys.* **2011,** *131*, 223.
6. Qian, X. F.; Yin, J.; Huang, J. C.; Yang, Y. F.; Guo, X. X.; Zhu, Z. K. *Mater. Chem. Phys.* **2001,** *68*, 95.
7. Wang, H.; Fang, P.; Chen, Z.; Wang, S. *Appl. Surf. Sci.* **2007,** *253*, 8495.
8. Yang, C. C.; Li, Y. J.; Liou, T. *Desalination* **2011,** *276*, 366.
9. Paranhos, C. M.; Dahmouche, K.; Zaioncz, S.; Soares, B.; Pessan, L. A. *J. Polym. Sci. Part. B: Polym. Phys.* **2008,** *46*, 2618.
10. Yang, C. C.; Lee, Y. J. *Thin Solid Films* **2009,** *517*, 4735.
11. Morimune, S.; Kotera, M.; Nishino, T.; Goto, K.; Hata, K. *Macromolecules* **2011,** *44*, 4415.
12. Zhu, Y.; Du, Z.; Li, H.; Zhang, C. *Polym. Eng. Sci.* **2011,** *51*, 1770.
13. Wang, J.; Wang, X.; Xu, C.; Zhangaand, M.; Shanga, X. *Polym. Int.* **2011,** *60*, 816.
14. Yoon, S. D.; Park, M. H.; Byun, H. S. *Carbohydr. Polym.* **2012,** *87*, 676.
15. Millon, L. E.; Oates, C. J.; Wan, W. *J. Biomed. Mater. Res. Part B: Appl. Biomater.* **2009,** *90B*, 922.
16. Lou, Y.; Liu, M.; Miao, X.; Zhang, L.; Wang, X. *Polym. Compos.* **2010,** *31*, 1184.
17. Guo, R.; Ma, X.; Hu, C.; Jiang, Z. *Polymer* **2007,** *48*, 2939.
18. Fernandesa, D. M.; Hechenleitnera, A. A. W.; Limab, S. M.; Andradeb, L. H. C.; Cairesc, A. R. L.; Pinedaa, E. A. G. *Mater. Chem. Phys.* **2011,** *128*, 375.
19. Gandhi, S.; Nagalakshmi, N.; Baskaran, I.; Dhanalakshmi, V.; Nair, M. R.; Anbarasan, R. *J. Appl. Polym. Sci.* **2010,** *118*, 1666.
20. Marten, L. F.; Famili, A.; Nangeroni, J. F. U. S. Pat. 5,051,222, **1991.**
21. Seymour, S.; Mitsuzo, S.; John J.R., M. Eur. Pat. 0,152,180, **1985.**
22. Maria, S.; Christer, B.; Pirjo, J.; Helge, L.; Anssi, L.; Bo, M. Eur. Pat. 0,389,695, **1990.**
23. Kuechler, M.; Reinhard, G. U.S. Pat. 5,324,572, **1994.**
24. Chen, N.; Li, L.; Wang, Q. *Plast. Rubber Compos.* **2007,** *36*, 283.
25. Jang, J.; Lee, D. *Polymer* **2003,** *44*, 8139.
26. Wang, R.; Wang, Q.; Li, L. *Polym. Int.* **2003,** *52*, 1820.
27. Mohsin, M.; Hossin, A.; Haik, Y. *J. Appl. Polym. Sci.* **2011,** *122*, 3108.
28. Alexya, P.; Lacĺkb, I.; Šimkováa, B.; Bakoš, D.; Prónayová, N.; Liptaj, T.; Hanzelová, S.; Várošová, M. *Polym. Degrad. Stab.* **2004,** *85*, 823.
29. Mark, H. F.; Kroschwitz, J. I. Encyclopedia of Polymer Science Engineering; Wiley: New York, **1986; 487.**
30. Xu, X.; Li, B.; Lu, H.; Zhang, Z.; Wang, H. *Appl. Surf. Sci.* **2007,** *254*, 1456.
31. Liu, X.; Wu, Q.; Berglund, L. A. *Polymer* **2002,** *43*, 4976.
32. Xiong, H. G.; Tang, S. W.; Tang, H. L.; Zou, P. *Carbohydr. Polym.* **2008,** *71*, 263.

33. Assendert, H. E.; Windle, A. H. *Polymer* **1998,** *39*, 4295.
34. Sarkar, M. D.; Deb, P. *Adv. Polym.Tech.* **2008,** *27*, 152.
35. Luo, F.; Zhang, X.; Li, R.; Li, R.; Fu, D.; Gan, Z.; Ji, J.; Wang, D. *Acta Polym. Sin.* **2009,** *10*, 1043.
36. Lu, H.; Xu, X.; Li, X.; Zhang, Z. B. *Mater. Sci.* **2006,** *29*, 485.
37. Preghenella, M.; Pegoretti, A.; Migliaresi, C. *Polymer* **2005,** *46*, 12065.
38. Wu, W.; Xu, Z. *Acta Polym. Sin.* **2000,** *1*, 99.
39. Tjong, S. C.; Li, R. K. Y.; Cheung, T. *Polym. Eng. Sci.* **1997,** *37*, 166.
40. Nath, D. C. D.; Bandyopadhyay, S.; Boughton, P.; Yu, A.; Blackburn, D.; White, C. *J. Appl. Polym. Sci.* **2010,** *117*, 117.
41. Tang, S.; Zou, P.; Xiong, H.; Tang, H. *Carbohydr. Polym.* **2008,** *72*, 521.
42. Tang, H.; Xiong, H.; Tang, S.; Zou, P. *J. Appl. Polym. Sci.* **2009,** *113*, 34.